Brief Report

Doppler LiDAR Observation of Subsidence in Synoptic Scale and Performance of a Global Numerical Weather Prediction Model in Capturing the Subsidence

Pak-Wai Chan [1,*], Steve Hung-Lam Yim [2,3,4] and Tao Huang [5]

1   Hong Kong Observatory, Hong Kong, China
2   Asian School of the Environment, Nanyang Technological University (NTU), Singapore 639798, Singapore
3   Lee Kong Chian School of Medicine, Nanyang Technological University (NTU), Singapore 639798, Singapore
4   Earth Observatory of Singapore, Nanyang Technological University (NTU), Singapore 639798, Singapore
5   Department of Geography and Resource Management, The Chinese University of Hong Kong, Hong Kong, China
*   Correspondence: author: pwchan@hko.gov.hk

Abstract: The vertical velocity data from a Doppler LiDAR situated at the centre of Hong Kong were examined to look for signature of subsidence within the atmospheric boundary layer against a synoptic background. Two case studies were performed, namely, stable atmospheric conditions in foggy weather and possible "subsidence heating" at the periphery of the outer circulation of an intense tropical cyclone. The LiDAR's Doppler velocity data were found to provide insights into the vertical motion of the air on the synoptic scale. They appear to confirm subsidence in foggy weather but provide new information about the mechanism for the occurrence of extremely hot weather. The data were also compared with vertical velocity forecasts from a numerical weather prediction model to assess the quality of the forecast. The Doppler LiDAR's vertical velocity data were found to be useful in the verification of omega forecasts from the global numerical weather prediction model. They were found to provide further insights into the subsidence of the troposphere, particularly the atmospheric boundary layer, in certain synoptic patterns.

Keywords: Doppler LiDAR; vertical velocity; ECMWF

1. Introduction

Subsidence on the synoptic scale has often been referenced in the formulation of weather forecasts and in explanations of local weather in subtropical coastal cities such as Hong Kong [1–3]. Examples of this subsidence include the suppression of vertical mixing in the formation of coastal fog in the springtime and adiabatic heating associated with subsidence in the outer periphery of tropical cyclones in contributing to extremely hot weather in the summer (defined as temperatures of 35 °C or above) [4]. However, direct observations of subsidence were not available in the past, and it was uncertain if these weather features were related to the downward motion within the atmospheric boundary layer. In addition, it was also not confirmed if global numerical weather prediction (NWP) models were performing well or not in capturing the vertical motion of the air in such weather conditions due to the lack of actual observations.

The installation of a Doppler Light Detection and Ranging (LiDAR) system in King's Park, Hong Kong has offered the opportunity for continuous observations of vertical motion of the air in the urban areas of the region since 2019. This instrument has been demonstrated in a past study in providing unprecedented observations of updrafts within the atmospheric boundary layer [5]. Vertical subsidence of the air would be another interesting topic to be explored with the aid of Doppler LiDAR. Such observational data may also be compared with a vertical motion forecast by an NWP model to confirm if the

numerical model can capture synoptic scale subsidence. In the present paper, direct model outputs from the integrated forecast system (IFS) based on the deterministic model used by the European Centre for Medium-Range Weather Forecasts (ECMWF) were considered.

Doppler LiDAR systems have been employed in many applications, particularly including aviation. This paper is novel in its application of vertical velocity data from Doppler LiDAR in studying subsidence in synoptic patterns and its relationship with foggy weather and very hot weather. The case studies will shed new light on the application of LiDAR in such weather conditions.

In the following sections, synoptic patterns and local weather observations are described first, followed by a brief overview of the vertical motion data from Doppler LiDAR observations. The vertical velocity simulated per the ECMWF's model at the grid point near King's Park is extracted and later examined to see if the subsidence is well captured by the numerical model.

2. Data and Method

2.1. Doppler LiDAR at KP, Hong Kong

The Doppler LiDAR system, denoted as LiDAR KP in this study, was situated at the King's Park Meteorological Station (KPMS, 22.311° N, 114.173° E) in the central area of Hong Kong, China. The site is under the administration of the Hong Kong Observatory (HKO) and serves as the single upper-air sounding station in Hong Kong. LiDAR KP has formed an integral component of the 3DREAMS project since 2019. Detailed information regarding the sites can be found in prior published studies focusing on 3DREAMS in Hong Kong [5]. Vertical velocity data were obtained from the Stare mode of the LiDAR system, which measured radial Doppler velocity at an elevation angle of 90 degrees and at a temporal resolution of ~1 s. The range gate of the system was set at 30 m, with the maximum detecting range at 3000 m above ground level. The horizontal components of the wind were obtained from rotating the laser beam in a circle. Combined with synergetic observations, such as radiosonde sounding and rainfall record at KPMS, data obtained on rainy days were removed, and the performance of the LiDAR (horizontal wind speed and direction) were validated.

2.2. ECMWF Forecast Data

NWP data were derived from an IFS at the ECMWF [6], which is famous for its provision of highly advanced and precise weather predictions in Europe and its neighbouring regions. Intended to provide the state-of-the-art forecasting of atmospheric status, the ECMWF's forecast data provide an extensive overview of atmospheric conditions up to 15 days in advance. Notably, the ECMWF's forecasting models cover the entire global scale, with a particular emphasis on Europe, ensuring a holistic perspective on weather patterns that can impact the continent. Its performance on other continents has also been investigated in other studies [7–9]. The ECMWF employs high-resolution numerical weather prediction models, which enable highly accurate and finely detailed forecasting, which is particularly beneficial for the varying and densely populated regions of Europe. Furthermore, the ECMWF produces ensemble forecasts, offering a spectrum of potential weather scenarios that shed light on the uncertainty associated with the forecasts. This contributes significantly to decision-making and risk assessment. The ECMWF data include a wide range of parameters, encompassing variables such as temperature, precipitation, wind speed, etc. These parameters find applications in a diverse array of fields, spanning agriculture to disaster preparedness, underscoring the versatility and utility of the ECMWF's offerings [10–13]. Vertical velocity (hPa/s) data used in this study were derived from the specific KP grid from the ECMWF's IFS.

2.3. Synoptic Weather Chart

A synoptic weather chart covering Hong Kong and South China is published by the HKO every 6 h. Synoptic weather systems such as fronts and tropical cyclones can also

be observed on the weather chart. Data can be accessed directly from the HKO's website (https://www.hko.gov.hk/en/wxinfo/currwx/wxcht.htm (accessed on 1 August 2023)).

Below, the vertical components of the wind from the Doppler LiDAR were compared with the vertical velocity forecast from the numerical weather prediction model. The synoptic patterns of the cases under study are shown on the synoptic surface weather charts.

3. Results and Discussion

3.1. Synoptic Weather Patterns and Local Observations

Two cases were considered in the present paper. The first case was about foggy weather for two days in February 2023. The isobaric charts on the synoptic scale for this case are presented in Figure 1. On 11 February 2023 (Figure 1a), a ridge of high pressure existed along the southeastern coast of China, bringing a moderate easterly wind to the coast of Guangdong Province. The ridge collapsed in the next two days, so that on 13 February (Figure 1b), the isobars near the coast of Guangdong were reduced. At the same time, a cold front existed in the inland areas of South China. These synoptic weather patterns were favourable for the occurrence of foggy weather in Hong Kong, especially in the morning.
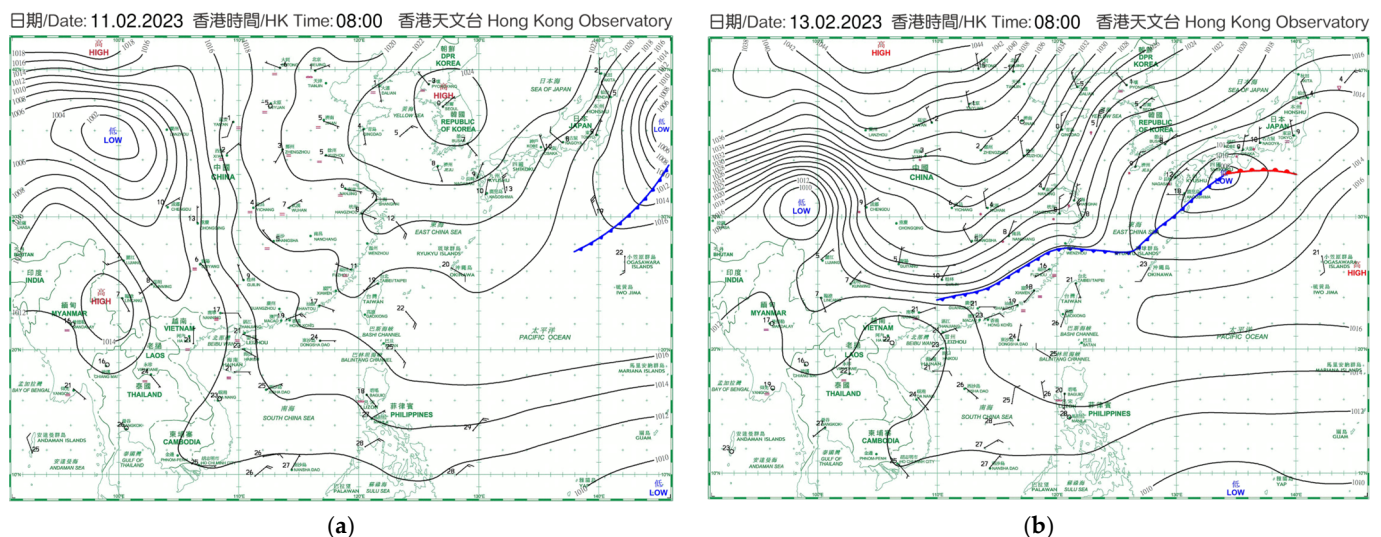

| (a) | (b) |

Figure 1. Surface isobaric chart for 8 a.m. local time, Hong Kong (UTC + 8), on (**a**) 11 February 2023 and (**b**) 13 February 2023. Blue line refers to the position of cold front. Red line refers to the position of warm front.

The local weather observations at selected times on these two days are shown in Figure 2. Light to moderate easterly winds existed over Victoria Harbour on the first day (Figure 2a). On the second day (Figure 2b), the local winds were even lighter and more variable. The light wind conditions were conductive to the occurrence of fog.

The second case refers to possible subsidence at the outer periphery of the circulation of a tropical cyclone near Taiwan; such subsidence is typical during the occurrence of extremely hot weather in Hong Kong. The synoptic patterns on the surface can be found in Figure 3. In this period of 2 days (26 to 27 July 2023), Super Typhoon Doksuri over the Luzon Strait moved slowly to the northwest. Hong Kong was situated in the outer circulation of this intense tropical cyclone system. It is believed that the subsidence in the outer periphery of an intense cyclone caused very hot weather over the region.

The local weather conditions for the second case on these two days can be found in Figure 4. Winds were mainly light to moderate and westerly to north-westerly over the territory. Advection of hotter air from the heated continent to the north of Hong Kong can be one of the possible reasons for high temperatures in Hong Kong. However, it was not clear from the surface observations if there was subsidence in the atmospheric boundary layer.
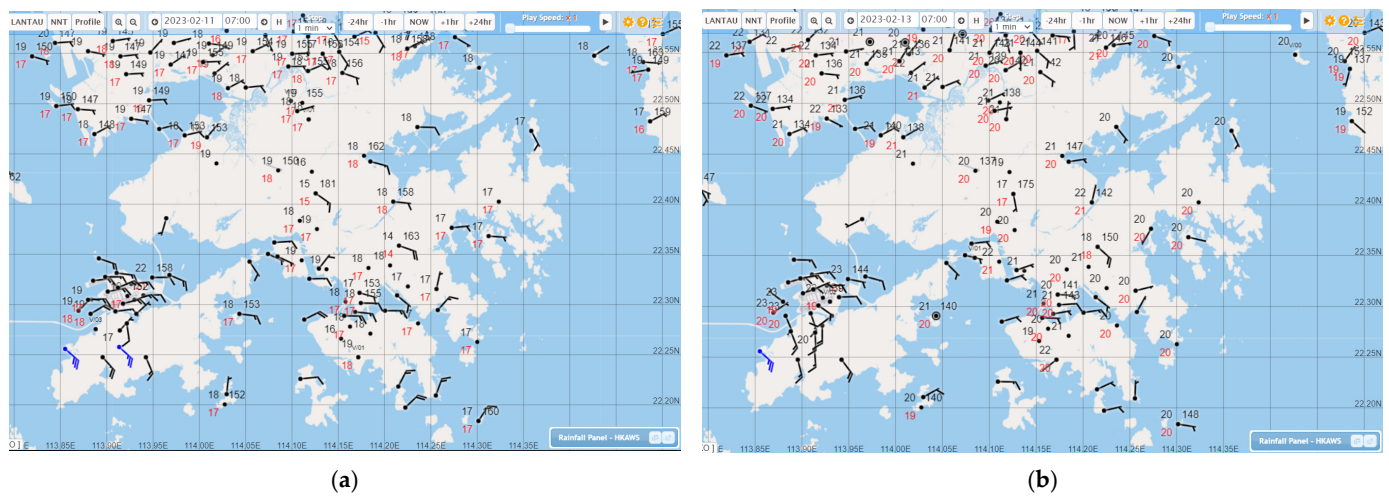
Figure 2. The surface observations in Hong Kong at 7 a.m. local time on (**a**) 11 February 2023 and (**b**) 13 February 2023.
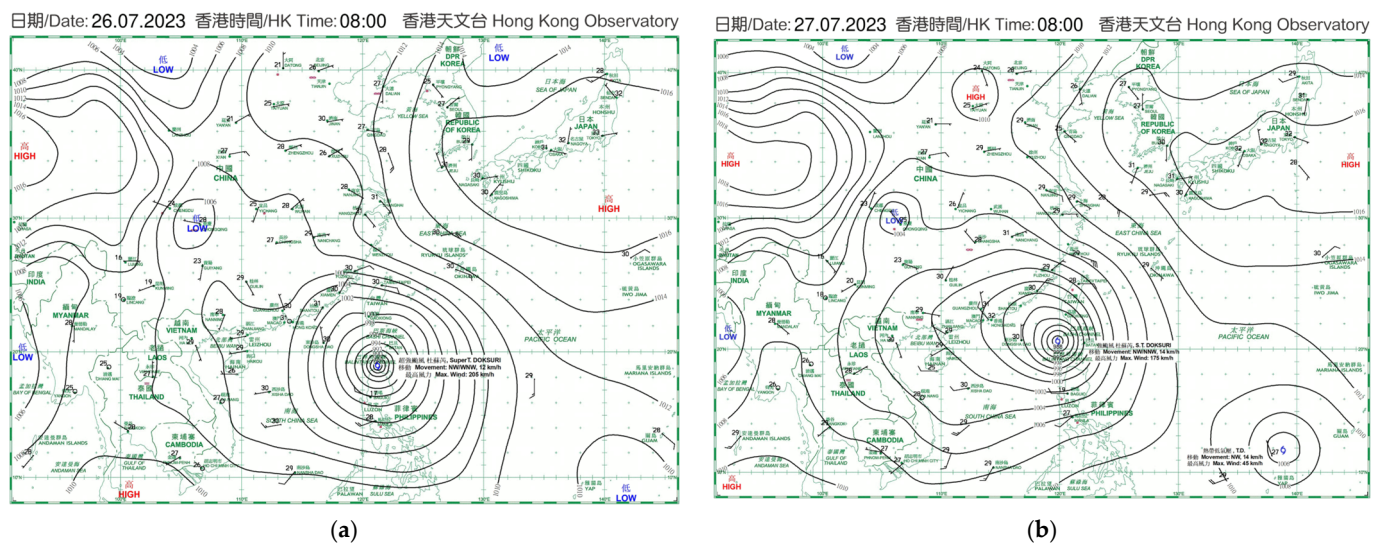

Figure 3. Same as Figure 1 but for (**a**) 26 July 2023 and (**b**) 27 July 2023.
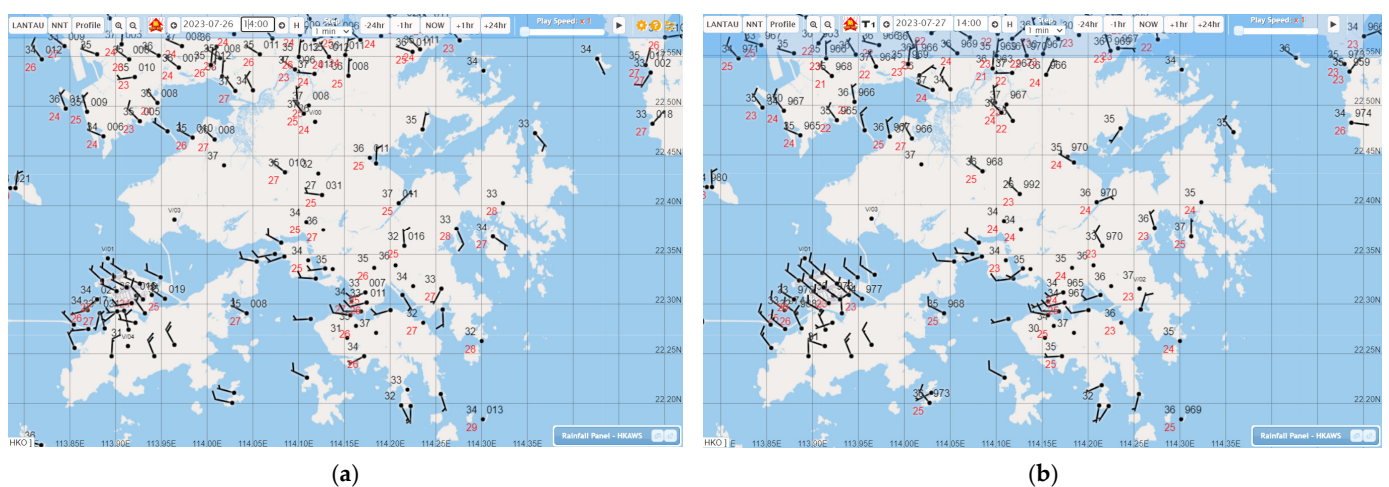

Figure 4. Same as Figure 2 but for 2 p.m. local time in Hong Kong on (**a**) 26 July 2023 and (**b**) 27 July 2023.

3.2. Doppler LiDAR Observation of Vertical Velocity

Vertical velocity data (time–height cross-section) for Doppler LiDAR at King's Park, Hong Kong were examined in the present section. For the first case in Figure 5, due to the low cloud cover, the measurement range of the LiDAR in the vertical was very much limited, mostly on the order of 200 to 300 m above ground. Figure 5a shows that the vertical velocity was mostly negative over the whole study period for this case, reaching about 1 to 2 m/s downward. This is the first time that downward vertical motion has been confirmed and documented during foggy weather in Hong Kong. The subsidence helped suppress vertical motion of the air, and thus the foggy conditions persisted over the waters of Hong Kong, making the fog rather hard to disperse. The vertical velocity data from LiDAR could be helpful to weather forecasters in monitoring low visibility weather.
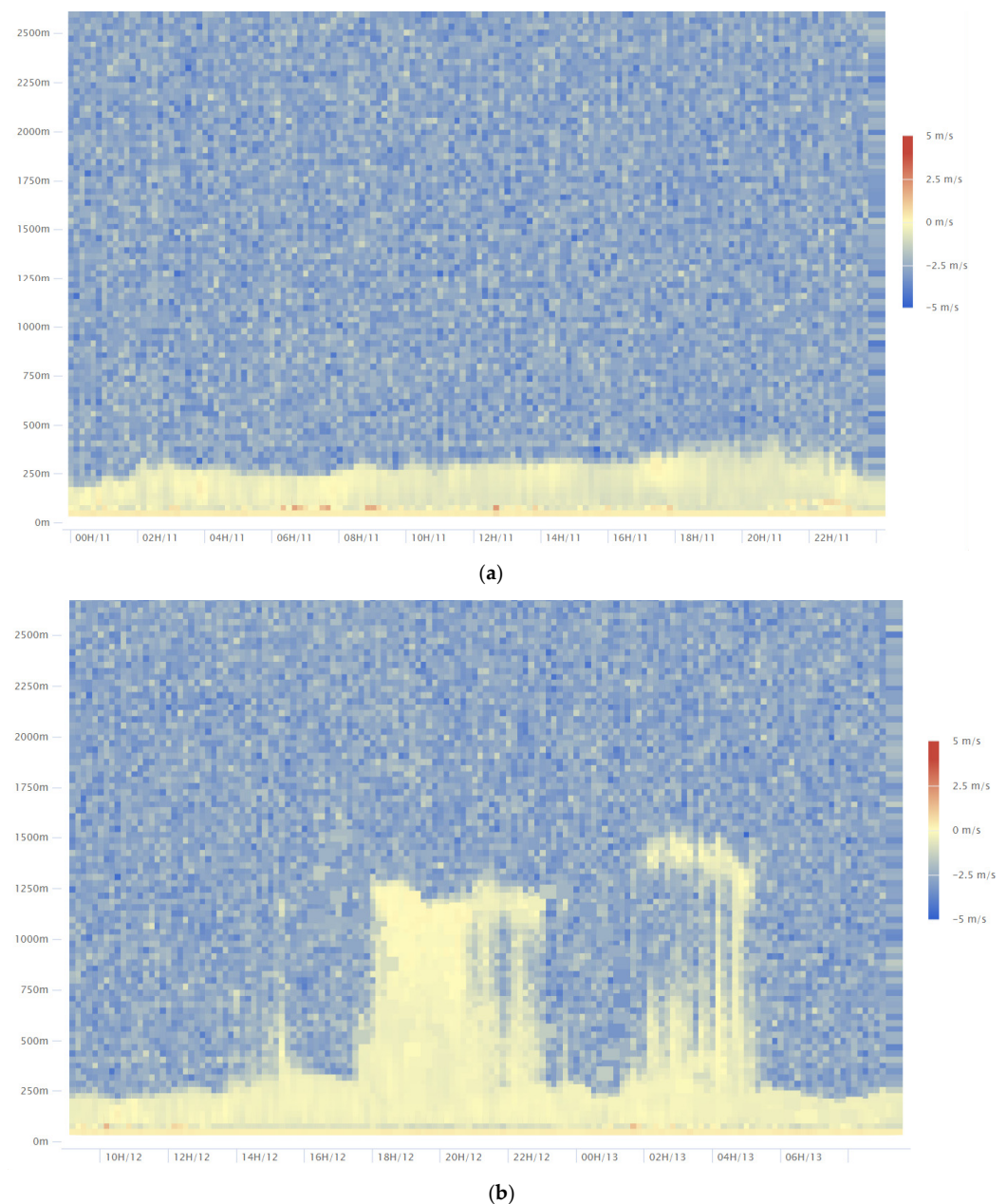

(a)

(b)

Figure 5. Time–height plot of the vertical velocity data from the Doppler LiDAR on (**a**) 11 February 2023 and (**b**) 12 to 13 February 2023. Warm colours indicate updrafts and cool colours indicate downdrafts. Times are in local time in Hong Kong (UTC + 8).

In the second case, the vertical motion was a little bit trickier. On the first day (Figure 6a), during the daytime, downward motion of 1 to 2 m/s was mostly observed below 700 m or so. There could have been sometimes during the day when upward vertical motion was detected by the LiDAR above that height, but the mostly downward motion within the atmospheric boundary layer appeared to confirm that subsidence was conducive to the heating up of the surface layer air, thus achieving a higher surface temperature during the day, at least for the conditions on 26 July 2023.
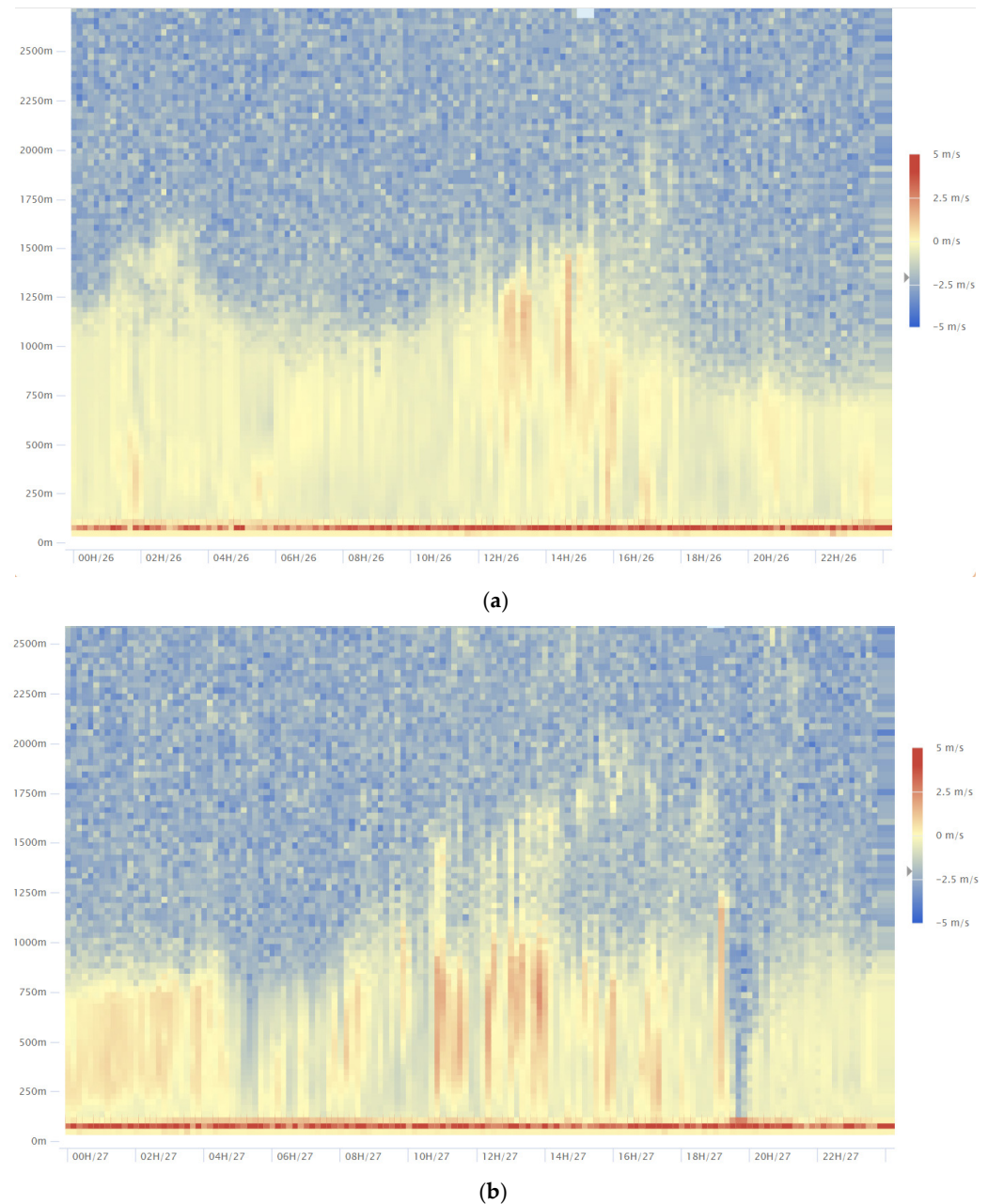

(a)

(b)

Figure 6. Time–height plot of the vertical velocity data from the Doppler LiDAR on (**a**) 26 July and (**b**) 27 July 2023. Warm colours indicate updrafts and cool colours indicate downdrafts. Times are in local time in Hong Kong (UTC + 8).

However, on the following day (27 July 2023), the vertical motion during the day as detected by the LiDAR appeared to be a mix of up- and downdrafts (Figure 6b), more consistent with the observations of vertical motion in the atmospheric boundary layer over a heated surface as commonly reported in the literature. It is not so clear if subsidence was really favouring the heating of the surface air. Therefore, the use of subsidence associated

with the outer circulation of an intense tropical cyclone may not be an appropriate explanation for the extremely high temperature on that day. On the other hand, advection of hotter air from the inland area may be a more suitable reason to explain the high temperatures. It can be seen from this example that vertical motion data from Doppler LiDAR offered more direct explanations of high temperatures in Hong Kong.

3.3. Performance of a Global NWP Model

With the availability of the vertical motion data from the Doppler LiDAR as the basis, we extended the study further by considering the capability of a global NWP model in capturing vertical motion on a synoptic scale. The time–height cross-section of ECMWF vertical velocity data at the location near King's Park, Hong Kong for the first case is shown in Figure 7. In the foggy weather case, the vertical motion was forecast to be mostly downward at this location, including the daytime period, which is consistent with the Doppler LiDAR observations. In particular, the horizontal distribution of vertical motion at 950 hPa is shown in Figure 8. Downward motion has been mostly forecast along the coast, particularly for the lighter wind day of 13 February 2023. This is consistent with the occurrence of widespread fog along the coast of southern China.
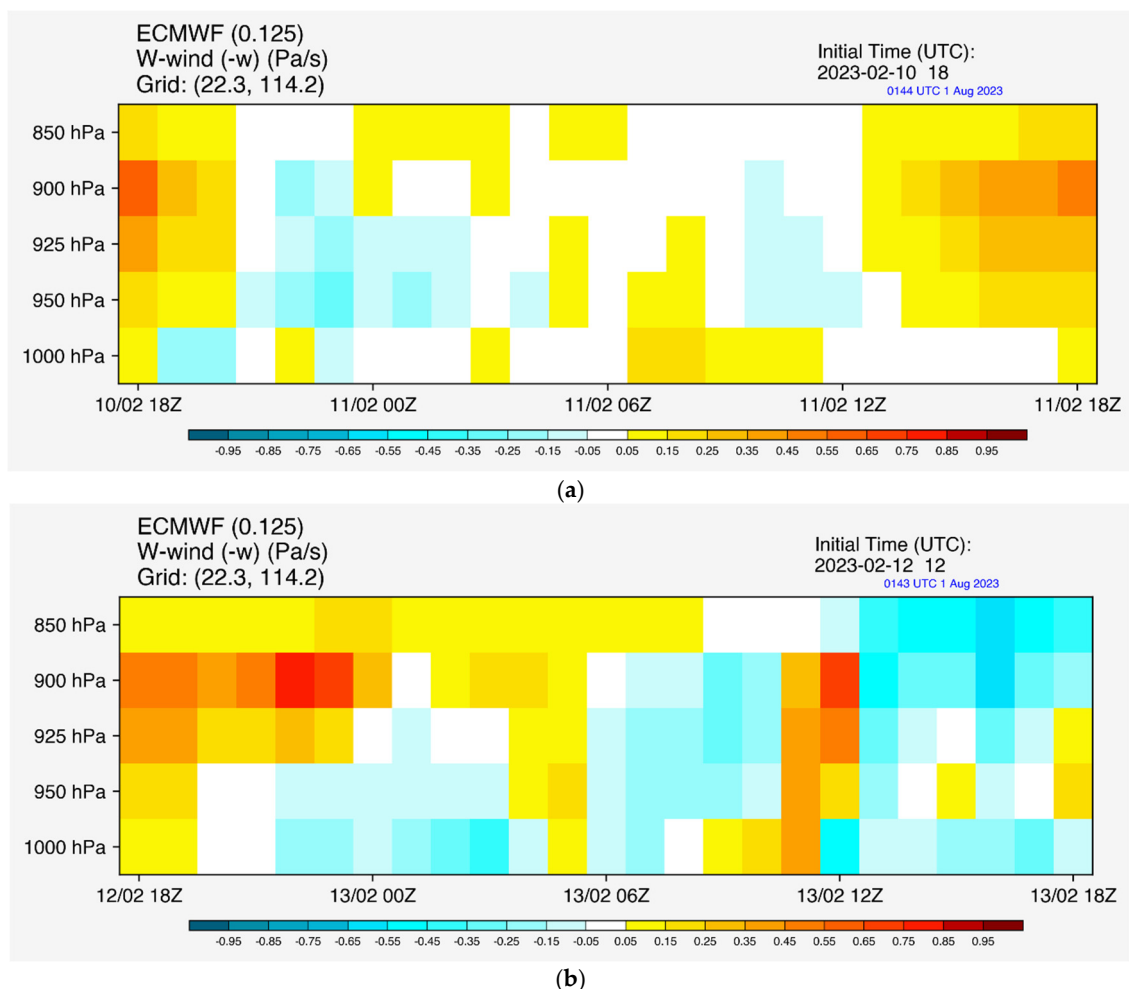

(**a**)

(**b**)

Figure 7. Vertical velocity (negative omega in Pa/s) at a grid point near King's Park, Hong Kong for (**a**) 11 February 2023 and (**b**) 13 February 2023. Warm colours indicate updrafts and cool colours indicate downdrafts. The times are in UTC (UTC + 8).

For the second case, on the first day (26 July 2023, Figure 9a), downward motion was forecast to occur for a while during the day at King's Park, though the vertical motion was mostly updrafts in the earlier part of the day. It appears that, within the model, the heating

of the surface air during the earlier part of the day might not have arisen mostly from subsidence in the atmospheric boundary layer. For the second day (27 July 2023, Figure 9b), the vertical motion was basically updrafts during the whole daytime period within the atmospheric boundary layer. Subsidence does not appear to be the major reason for the forecast occurrence of extremely hot weather. The 950 hPa vertical velocity in the region around Hong Kong is shown in Figure 10. In general, it is hard to discover a pattern of the horizontal distribution of vertical velocity in the daytime. It appears that updrafts may mostly occur along the coast. In inland areas, the pattern is basically a mixture of both updraft and downdraft. Thus, the model forecast may be more consistent with the vertical motion expected from a heated surface, without a clearly identifiable pattern.
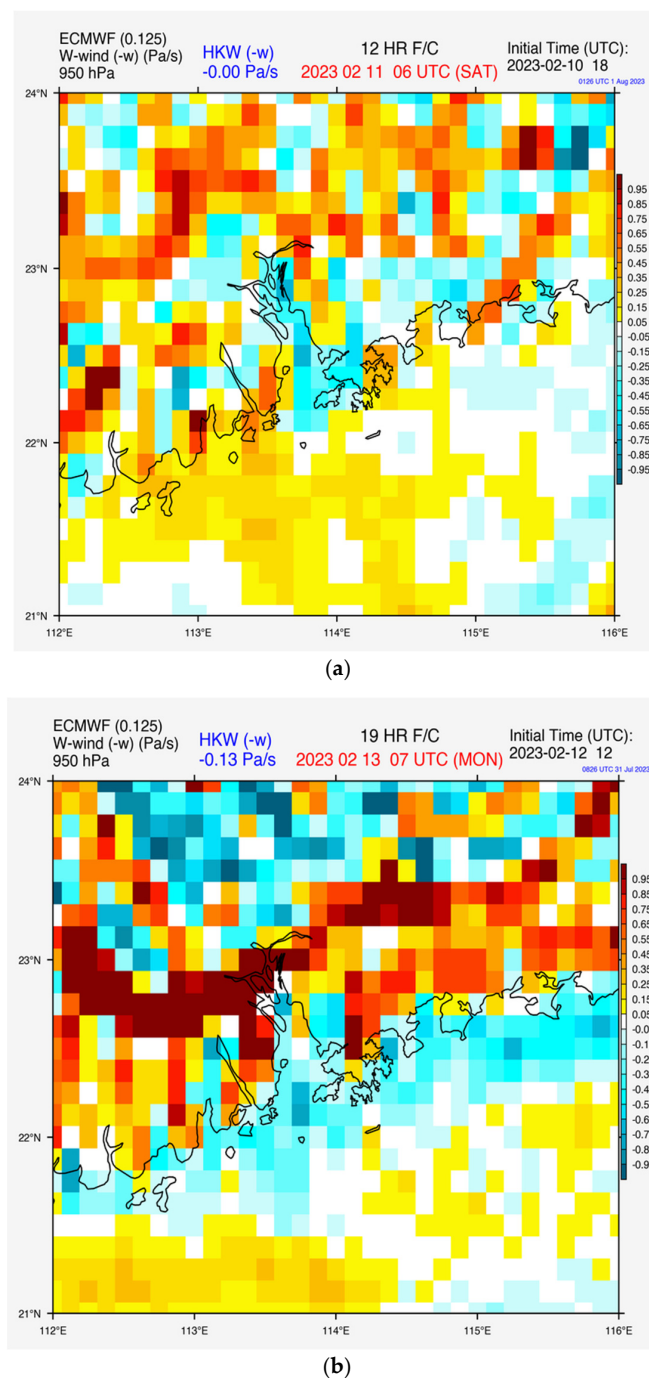

(**a**)

(**b**)

Figure 8. Vertical velocity of a numerical weather prediction model at 950 hPa. The colouring scheme is the same as Figure 7.
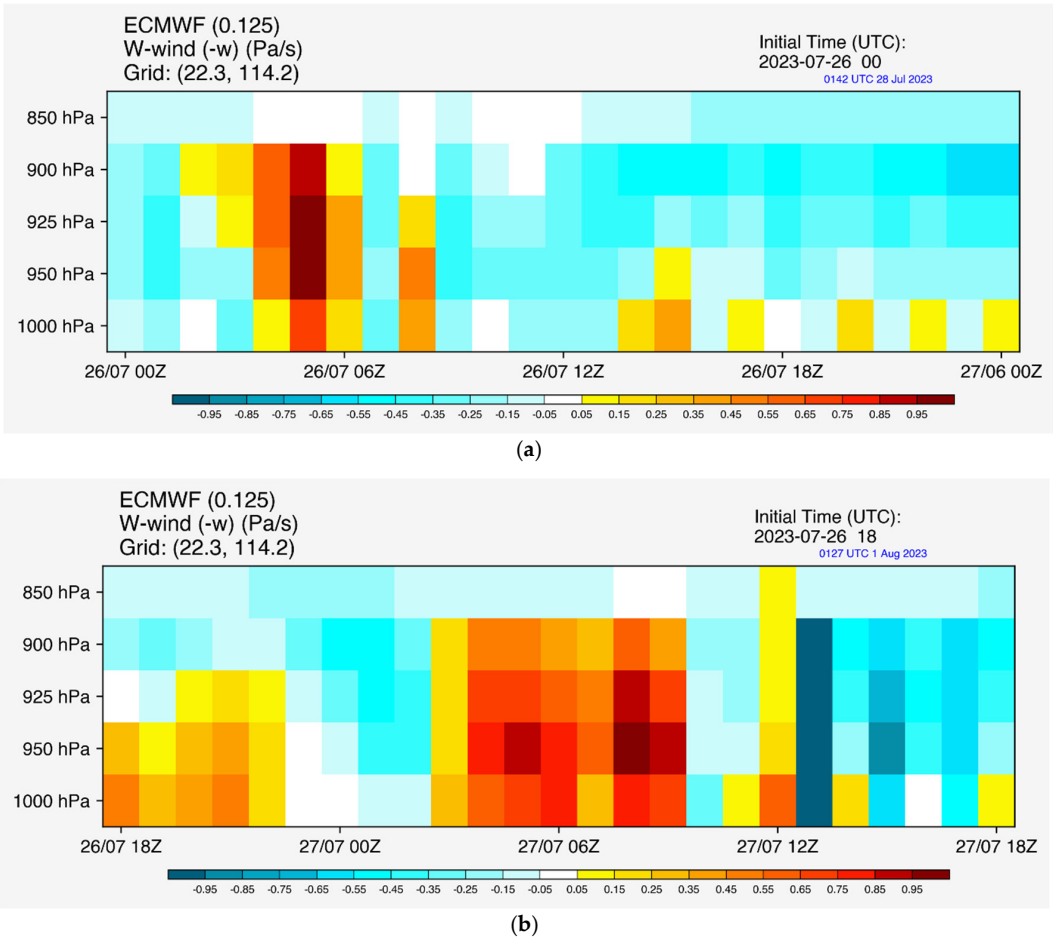
(**a**)

(**b**)

Figure 9. Same as Figure 7 but for (**a**) 26 July 2023 and (**b**) 27 July 2023.
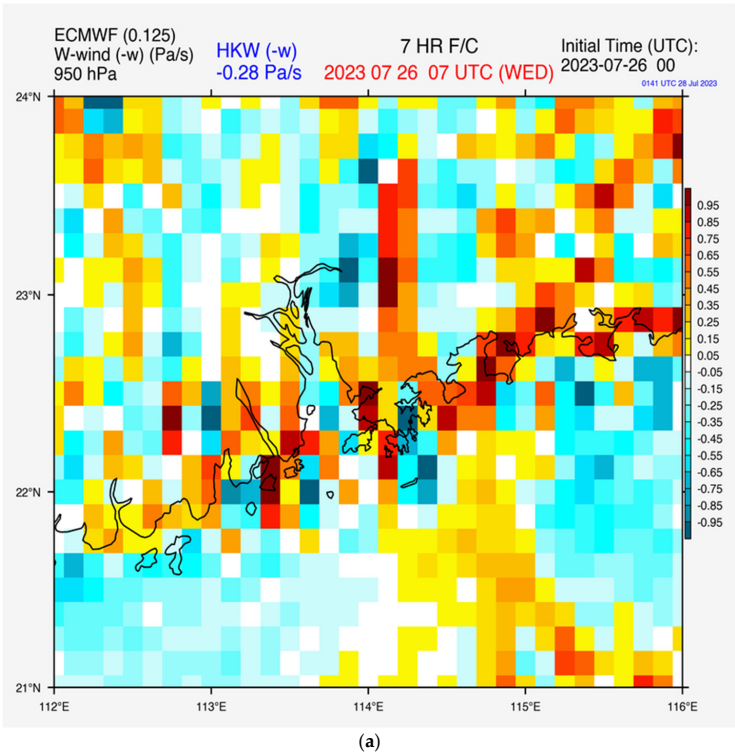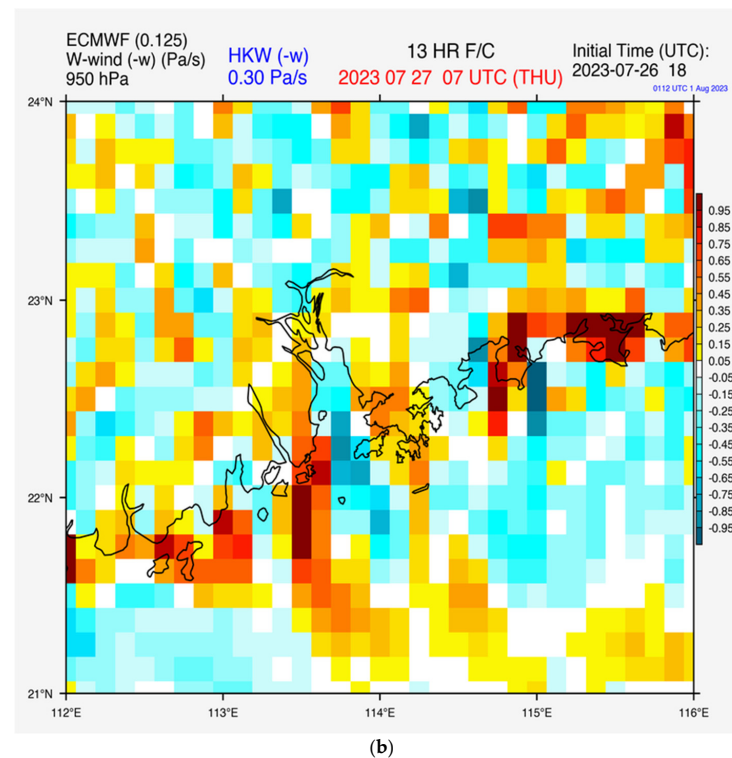

(**a**)

Figure 10. *Cont.*

(b)

Figure 10. Same as Figure 8 but for (**a**) 26 July 2023 and (**b**) 27 July 2023.

In the existing literature, there has been little discussion about the performance of vertical velocity in the global NWP model, especially over southern China, in comparison with the actual observations from LiDAR. This paper serves as the first of this kind of study, and we hope that it will stimulate further research in this direction.

4. Conclusions

The vertical motion data from a Doppler LiDAR station in Hong Kong were studied for the first time for suspected subsidence cases, namely, foggy weather in spring and "subsidence heating" in summer. Subsidence is indeed observed for fog. On the other hand, the reason for extremely hot weather could be a mix. It is not clear whether "subsidence heating" is indeed the true reason for high temperatures in Hong Kong all the time.

The Doppler velocity data were also compared with the predictions from an NWP model. In general, the downward motion in foggy weather was well captured in the model. For the summer case, however, the high temperature may occur because of multiple factors, not just attributable to subsidence heating alone. This gives new insight into the extremely hot weather in Hong Kong. The vertical velocity data from Doppler LiDAR provide the "sky truth" for verification of omega forecasts from numerical weather prediction models. This was found to be very useful in the model verification and provides new insights into subsidence motion in southern China.

Another potential application of Doppler LiDAR's vertical velocity is the monitoring and prediction of low air quality situations in southern China. Cases would be collected in this regard in order to see the performance of LiDAR in such weather conditions.

With the prolonged period of operation of Doppler LiDAR, more observational data from the instrument are being explored. Statistical analysis of vertical velocity in an urban area may be considered for reporting in the future.

References

1. Bellamy, J.C. Objective Calculations of Divergence, Vertical Velocity and Vorticity. *Bull. Am. Meteorol. Soc.* **1949**, *30*, 45–49. [CrossRef]
2. Blay-Carreras, E.; Pino, D.; Vilà-Guerau de Arellano, J.; van de Boer, A.; De Coster, O.; Darbieu, C.; Hartogensis, O.; Lohou, F.; Lothon, M.; Pietersen, H. Role of the Residual Layer and Large-Scale Subsidence on the Development and Evolution of the Convective Boundary Layer. *Atmos. Chem. Phys.* **2014**, *14*, 4515–4530. [CrossRef]
3. Berg, L.K.; Newsom, R.K.; Turner, D.D. Year-Long Vertical Velocity Statistics Derived from Doppler Lidar Data for the Continental Convective Boundary Layer. *J. Appl. Meteor. Climatol.* **2017**, *56*, 2441–2454. [CrossRef]
4. Li, P.; Fu, G.; Lu, C.; Fu, D.; Wang, S. The Formation Mechanism of a Spring Sea Fog Event over the Yellow Sea Associated with a Low-Level Jet. *Weather. Forecast.* **2012**, *27*, 1538–1553. [CrossRef]
5. Yim, S.H.L. Development of a 3D Real-Time Atmospheric Monitoring System (3DREAMS) Using Doppler LiDARs and Applications for Long-Term Analysis and Hot-and-Polluted Episodes. *Remote Sens.* **2020**, *12*, 1036. [CrossRef]
6. Isaksen, L.; Bonavita, M.; Buizza, R.; Fisher, M.; Haseler, J.; Leutbecher, M.; Raynaud, L. Ensemble of Data Assimilations at ECMWF. 2010. Available online: https://www.ecmwf.int/en/elibrary/74969-ensemble-data-assimilations-ecmwf (accessed on 1 August 2023).
7. Albergel, C.; de Rosnay, P.; Balsamo, G.; Isaksen, L.; Muñoz-Sabater, J. Soil Moisture Analyses at ECMWF: Evaluation Using Global Ground-Based In Situ Observations. *J. Hydrometeorol.* **2012**, *13*, 1442–1460. [CrossRef]
8. Liu, J.; Huang, J.; Chen, B.; Zhou, T.; Yan, H.; Jin, H.; Huang, Z.; Zhang, B. Comparisons of PBL Heights Derived from CALIPSO and ECMWF Reanalysis Data over China. *J. Quant. Spectrosc. Radiat. Transf.* **2015**, *153*, 102–112. [CrossRef]
9. Slingo, J.M. The Development and Verification of A Cloud Prediction Scheme For the Ecmwf Model. *Q. J. R. Meteorol. Soc.* **1987**, *113*, 899–927. [CrossRef]
10. Reed, R.J.; Klinker, E.; Hollingsworth, A. The Structure and Characteristics of African Easterly Wave Disturbances as Determined from the ECMWF Operational Analysis/Forecast System. *Meteorol. Atmos. Phys.* **1988**, *38*, 22–33. [CrossRef]
11. Klein, S.A.; Jakob, C. Validation and Sensitivities of Frontal Clouds Simulated by the ECMWF Model. *Mon. Weather. Rev.* **1999**, *127*, 2514–2531. [CrossRef]
12. Belo-Pereira, M. Comparison of In-Flight Aircraft Icing Algorithms Based on ECMWF Forecasts. *Meteorol. Appl.* **2015**, *22*, 705–715. [CrossRef]
13. Gisinger, S.; Polichtchouk, I.; Dörnbrack, A.; Reichert, R.; Kaifler, B.; Kaifler, N.; Rapp, M.; Sandu, I. Gravity-Wave-Driven Seasonal Variability of Temperature Differences Between ECMWF IFS and Rayleigh Lidar Measurements in the Lee of the Southern Andes. *J. Geophys. Res. Atmos.* **2022**, *127*, e2021JD036270. [CrossRef]